*Catalysts* **2013**, *3*, 599-613; doi:10.3390/catal3030599

OPEN ACCESS

*catalysts*

**ISSN 2073-4344**

www.mdpi.com/journal/catalysts

*Article*

# Fabrication and Catalytic Activity of Thermally Stable Gold Nanoparticles on Ultrastable Y (USY) Zeolites

**Takashi Sanada [1,2], Chika Murakami [1], Kinga Góra-Marek [3], Keiko Iida [2], Naonobu Katada [1] and Kazu Okumura [1,*]**

[1] Department of Chemistry and Biotechnology, Graduate School of Engineering, Tottori University, 4-101 Koyama-cho Minami, Tottori 680-8552, Japan; E-Mails: sanada@nissan-arc.co.jp (T.S.); b07t4054c@yahoo.co.jp (C.M.); katada@chem.tottori-u.ac.jp (N.K.)

[2] Research Department, NISSAN ARC, LTD., Yokosuka 237-0061, Japan; E-Mail: iida@nissan-arc.co.jp

[3] Faculty of Chemistry, Jagiellonian University, Ingardena Street 3, 30-060 Krakow, Poland; E-Mail: kinga.goramarek@gmail.com

***** Author to whom correspondence should be addressed; E-Mail: okmr@chem.tottori-u.ac.jp; Tel.: +81-857-31-5257; Fax: +81-857-31-5684.

*Received: 22 April 2013; in revised form: 17 June 2013 / Accepted: 1 July 2013 / Published: 9 July 2013*

---

**Abstract:** Au was deposited on ultrastable Y (USY) zeolites using an ion-exchange method. Up to 5.5 wt% Au was introduced into the $NH_4$-form of USY zeolites. In contrast, deposition of Au hardly took place on the H- and Na-forms of Y-type zeolites, $NH_4$-forms of mordenite, and ZSM-5. Treatment of the Au-loaded USY zeolite in a $H_2$ atmosphere, afforded $Au^0$ nanoparticles. These particles were thermally stable even at 973 K, where their mean particle diameter was 3.7 nm. In contrast, highly aggregated Au particles were observed after thermal treatment at temperatures lower than 523 K, followed by storage in air for a month. The resulting particle sizes were in good correlation with the IR band intensity of the adsorbed CO and the catalytic activity of Au in the aerobic oxidation of benzyl alcohol. The Au nanoparticles showed highest activity when the Au/USY zeolite was thermally treated at 673–973 K. A negligible deactivation was observed after repeating the reaction at least 12 times. In the case of $Au/TiO_2$ catalyst prepared by the deposition-precipitation method, the highest activity was observed at 573 K, which was lower than the temperature used for the Au/USY zeolites. This study demonstrated the potential use of the $NH_4$-form of USY zeolites for supporting Au.

**Keywords:** gold cluster; nanoparticle; USY zeolite; Brønsted acid; partial oxidation

## 1. Introduction

Much attention has been paid to Au-loaded catalysts since the pioneering work done by Haruta and co-researchers [1,2]. It has been reported that the catalytic activity of Au nanoparticles is sensitive to the preparation method and the type of support because it depends strongly on the size and shape of the Au nanoparticles [3]. In particular, high catalytic activity has been reported for the Au particles smaller than several nanometers in size, not only in the research field of heterogeneous, but also in the homogeneous catalysts [4–6]. Earlier reports dealing with heterogeneous Au catalysts focused on the use of reducible metal oxides, such as $TiO_2$ as a support for Au. To date, several methods, including deposition-precipitation [7], chemical vapor deposition [8], and cation adsorption [9], have been applied for the preparation of $Au/TiO_2$ catalysts. Among these methods, deposition-precipitation has been the most frequently employed method for Au loading, and it involves the use of tetrachloroauric (III) acid as a precursor of Au. In this method, the pH of tetrachloroauric (III) acid solution was adjusted by an aqueous solution of ammonia, NaOH, and urea in the presence of supports such as $TiO_2$ [10,11]. On the other hand, the volume of research dealing with Au-loaded acidic supports is smaller than that on basic supports, possibly because the deposition of $AuCl_3$ on acidic supports was difficult in an aqueous alkaline solution that was otherwise employed for Au loading on $TiO_2$. Despite this challenge, several groups have reported the use of acidic zeolites as supports for Au. For instance, Au loaded on Y-type and HZSM-5 zeolites was used in the direct synthesis of hydrogen peroxide [12]. The $Au(en)_2Cl_3$ complex was supported on Y-type zeolites to obtain electron-deficient Au particles [13]. Au nanoparticles, accessible only through zeolite micropores, were reported to be active in the size-selective aerobic aldehyde oxidation [14]. Zeolites are promising supports for Au because of the presence of ion-exchange sites such as $NH_4^+$. It was expected that Au could be introduced into the $NH_4^+$-zeolite through the formation of $NH_4Cl$, providing a new and simple method for introducing Au into the zeolite by mixing a solution of $HAuCl_4$ and $NH_4^+$-zeolite without any special care. In other words, $Cl^-$ of $HAuCl_4$ was removed through the reaction with $NH_4^+$, unlike in the case of impregnated samples wherein $Cl^-$ remained on the support [15]. Other advantages of zeolite include high thermal stability, presence of large surface area, and micropores that may hinder the sintering of Au. Also, coalescence of Au may be thwarted by the wall structure of zeolite at high temperatures.

The purpose of this study is to establish a new method for the preparation of Au nanoclusters on zeolite supports and demonstrate that Au° nanoparticles having a narrow size distribution were obtained after calcination at >673 K. Here, ultrastable Y (USY) zeolites were predominantly employed as the supports for Au. The USY zeolites were prepared by the steam treatment of $NH_4^+$-Y, followed by reaction with an ammonium nitrate solution. The resulting ammonium-treated USY zeolites had strong Brønsted acid sites [16]. First, we developed a new method for loading Au onto $NH_4^+$-USY zeolites using an aqueous solution of $HAuCl_4$. Then, the as-prepared Au/USY zeolites were thermally treated in a $H_2$ atmosphere at 353–1073 K. The treated samples were characterized by X-ray diffraction (XRD), transmission electron microscopy (TEM), and infrared (IR) spectroscopy. Partial oxidation of

benzyl alcohol in the liquid phase was employed as a test reaction on the supported Au. This is because the oxidation of benzyl alcohol has received substantial attention as a probe molecule to test the selectivity and efficiency of novel metallic Au catalysts [17]. The catalytic activity and selectivity of Au nanoparticles were sensitive to the particle size and electronic state of Au [18]. The catalytic activity of the thermally treated Au/USY zeolite was correlated with the Au dispersion, as measured by XRD and TEM. The performance was compared with that of $Au/TiO_2$ catalyst prepared by the conventional deposition-precipitation method.

## 2. Results and Discussion

### *2.1. Loading of Au on Y-Type Zeolites*

Table 1 lists the values of Au loading as measured by inductively coupled plasma (ICP) after digestion of zeolite-supported Au with aqua regia. Most of the Au present in the mother liquor was introduced into the $NH_4^+$-Y, $CaNH_4^+$-Y, and $NH_4^+$-USY zeolites. Deposition of Au partially took place on β-type zeolite (1.8 wt%). In contrast, the amounts of Au on the $NH_4^+$-ZSM-5, $NH_4^+$-mordenite, and $Na^+$-Y zeolites were almost negligible. Probably, a supercage—a relatively large space with a diameter of 1.3 nm—was necessary to accommodate $HAuCl_4$ in Y-type zeolites.

**Table 1.** $Si/Al_2$ ratio and Au loading of Au/zeolites.

| Support | $Si/Al_2$ | Loading/wt% | Support | $Si/Al_2$ | Loading/wt% |
|---|---|---|---|---|---|
| $NH_4$-ZSM-5 | 90 | 0.1 | H-USY | 7.7 | 0.1 |
| $NH_4$-MOR | 15 | 0.1 | $NH_4$-Y | 5.5 | 3.1 |
| $NH_4$-beta | 20 | 1.8 | $NH_4$-CaY | 7.7 | 3.3 |
| Na-Y | 5.5 | 0.1 | $NH_4$-USY | 7.7 | 3.1 |

Figure 1 (▲) shows Au loading on USY zeolites that were thermally treated in a $N_2$ stream at different temperatures prior to Au loading. Approximately 3 wt% of Au was loaded onto the USY zeolites that had been treated at <523 K. The amount of Au loading decreased on increasing the temperature to 573 K. Only 0.1 wt% of Au was loaded onto the USY zeolite at 673–773 K. The amount of $NH_4^+$ was measured by the temperature programmed desorption of $NH_3$ at each temperature and plotted in Figure 1 (○). The amount of $NH_4^+$ in the USY zeolite decreased upon heating because of its decomposition into $NH_3$ and $H^+$. The amount of Au was closely related to that of $NH_4^+$. In other words, before ion exchange, Au loading decreased to approximately zero on thermally treating the USY zeolite at 723 K, where $NH_4^+$ was completely decomposed to yield the H-form zeolite. This indicated that $NH_4^+$ played an important role in the deposition of Au on the zeolite. Formation of $NH_4Cl$ (4 mol) was observed during the deposition of Au (1 mol) on the $NH_4$-USY zeolite, as verified by the IR, XRD, and temperature gravimetric analyses. This implied that the ion exchange of $HAuCl_4$ with $NH_4^+$ took place simultaneously with the formation of $NH_4Cl$. The Au $L_3$-edge extended X-ray absorption fine-structure (EXAFS) analysis revealed the presence of $Au_2O_3$ on the as-prepared samples, which suggested that the hydrolysis of $Au^{3+}$ proceeded to give $Au_2O_3$ on USY zeolites [19]. The maximum loading of Au on the $NH_4^+$-USY zeolite was 5.5 wt%, which was obtained by employing an excessive amount of $HAuCl_4$. When 5.5 wt% Au was introduced into the $NH_4^+$-USY

zeolite, 1.1 mol $kg^{-1}$ of $NH_4^+$ was eliminated to yield $NH_4Cl$, considering that the molar ratio of $NH_4^+$ and Au was 4. The amount (1.1 mol $kg^{-1}$) corresponded to 70% of the total amount of $NH_4^+$ (1.6 mol $kg^{-1}$) present in the $NH_4^+$-USY zeolite. The efficient loading of Au on the Y-type zeolite may be due to the presence of a high concentration of $NH_4^+$ (Brønsted acid sites) and a supercage having large pores that facilitated the reaction with $HAuCl_4$.

**Figure 1.** Dependence of $NH_4^+$ concentration in ultrastable Y (USY) zeolites and Au loading on thermal treatment temperature of $NH_4^+$-USY zeolites.

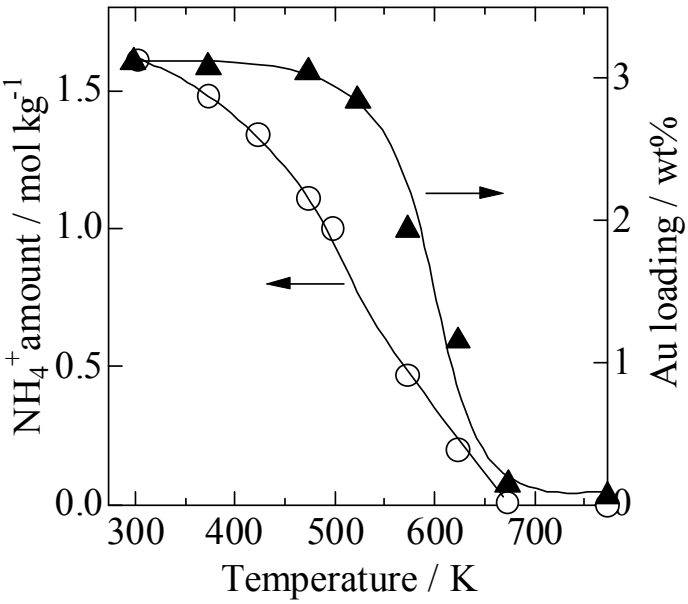


*2.2. XRD Patterns Measured under* Ex Situ *and* In Situ *Conditions*

Figure 2a shows the XRD patterns of a 3 wt%-Au/USY zeolite, which was first ion-exchanged with the $NH_4^+$-USY zeolite and then treated at different temperatures in the atmospheres of 6% $H_2$ diluted with Ar. The 6%-$H_2$ treated samples were stored in the dark for over one month in air prior to collecting the XRD data. The peaks at 2θ = 38.2° and 44.4° were due to diffractions from the (111) and (200) planes of Au°, respectively. Weak peaks assignable to the diffractions of FAU zeolite appeared at 38.1° and 44.2°, which overlapped with the diffractions from Au°. The intensity of reflections from the Au°(111) and Au°(200) planes increased with an increase in the treatment temperature, *i.e.*, from room temperature to 523 K. The appearance of steep reflections suggested the formation of aggregated crystals of Au metal. The intensity of these diffractions decreased and the peak became broader on further increasing the temperature, thereby suggesting a reduction in the particle size of Au. A marked reduction in peak intensity was observed at 573 K, indicating the formation of highly dispersed Au particles in the sample that was thermally treated at >573 K.

The data regarding the XRD patterns of the 3 wt%-Au/USY zeolites collected in an atmosphere of 3% $H_2$ under *in situ* conditions is depicted in Figure 2b. Broad diffractions due to the agglomerated Au particles were observed at ca. 38° and 44° in the XRD patterns of the Au/USY zeolites treated at 423–873 K. The change in the XRD patterns did not agree with those observed under *ex situ* conditions, *i.e.*, the intensity of diffractions decreased at >573 K. In order to understand the

contradiction between the data collected under *in situ* and *ex situ* conditions, the XRD patterns of the Au/USY zeolite stored in air were measured over a period of two months. Figure 3a shows the XRD patterns of the Au/USY zeolites treated at 473 K under a stream of 6% $H_2$ diluted with Ar, followed by storage in air at room temperature. The data was collected over a period of two months. Initially, the intensity of diffractions from Au°(111) and Au°(200) was small. The peaks gradually grew with time, and eventually, steep peaks were observed at 38.1° and 44.2° in the patterns of the Au/USY zeolites stored for 28–62 days. In contrast, no change was observed in the Au/USY zeolite treated at 773 K (Figure 3b). A significant difference between the samples treated at 473 and 773 K indicated that the temperature affected the change in the particle size of Au. Taking this into consideration, the appearance of steep peaks for the aggregated Au in Figure 2 (a, 423–523 K) was attributed to the growth of Au particles over a period of one month.

**Figure 2.** (**a**) XRD patterns of Au/USY zeolites treated at different temperatures under a 6% $H_2$ atmosphere diluted with Ar. Data was collected under *ex situ* conditions. Samples were stored in the dark for more than one month; (**b**) XRD patterns of Au/USY treated at different temperatures under a 3% $H_2$ atmosphere diluted with Ar. Data was collected under *in situ* conditions.

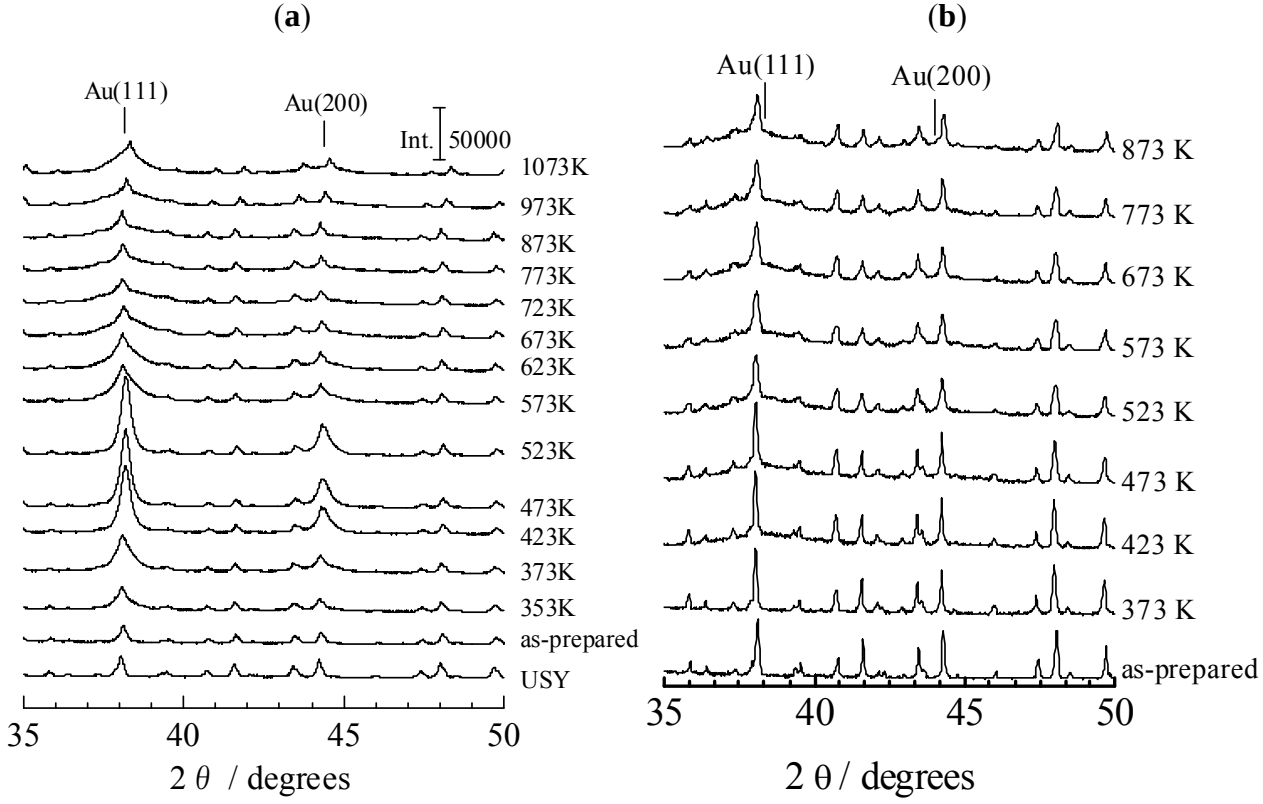


### *2.3. TEM Images of 3 wt%-Au/USY*

TEM analysis was employed to observe the Au particles on the Au/USY zeolites. The TEM image of the as-prepared 3 wt%-Au/USY zeolite is shown in Figure 4a. Small particles were found to be distributed in high concentration over the zeolite support. Figure 4b shows that the size distribution of

Au particles (presumably $Au_2O_3$ as found by XAFS [10]) was narrow, and the average diameter was 1.7 nm.

The TEM images and size distribution of the Au/USY zeolite treated at 473–1073 K under a 6% $H_2$ atmosphere are shown in Figures 5 and 6, respectively. The samples were stored in air for a month before conducting the TEM measurements. Large Au° particles of varying sizes were observed on the Au/USY treated at 473 K (Figure 5a). The shapes of the Au particles were not uniform. These observations agreed well with the XRD data in which steep reflections because of Au° appeared. In marked contrast, the Au° particles in the Au/USY treated at 773, 973 K, and 1073 K were much smaller and had homogeneous size distribution. It should be noted that the average size (1.8 nm) and distribution of the Au particles in the Au/USY treated at 773 K (Figure 6b) were close to those of the as-prepared Au/USY (Figure 4b). This suggested that the $Au_2O_3$ particles deposited on the $NH_4^+$-USY zeolite were reduced by $H_2$ to yield Au° particles without significant migration or coalescence. Although the average size of the Au particles became slightly larger after the thermal treatment at 973 K (3.7 nm), their size distribution still remained narrow. The average size of the Au particles in the Au/USY treated at 1073 K was 6.3 nm, which was slightly larger than that of the particles treated at 773–973 K, and the distribution also became broader. Possibly, the pores of the USY zeolite partially collapsed owing to the formation of Au° because the size of the Au particles was larger than that of the particles present in the USY zeolites.

**Figure 3.** XRD patterns of Au/USY zeolites treated at (**a**) 473 K and (**b**) 773 K in a stream of 6% $H_2$, followed by storage under atmospheric conditions at room temperature.

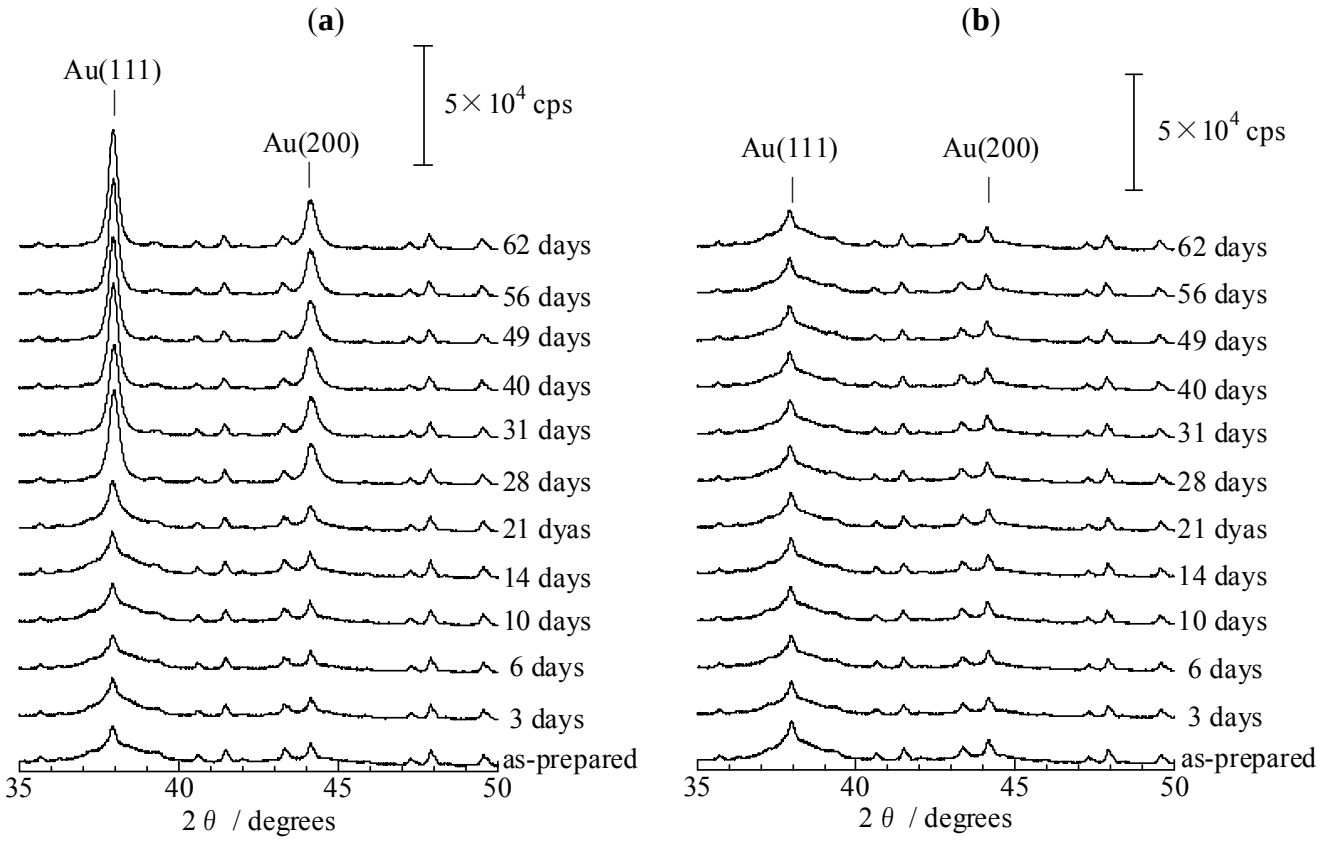

The mechanism of the coalescence of Au particles observed in the Au/USY zeolite treated at 473 K was not clear. One hypothesis was that the moisture present in air assisted the migration and growth of Au. In fact, the coalescence of Au nanoparticles was not observed in the 473 K-treated Au/USY zeolite when it was stored in dry air. Based on DFT calculations, it has been proposed that the coalescence of Au clusters could be prevented by anchoring them to the defective sites of $SiO_2$ [7]. Similarly, the OH groups generated on the defective sites in a moist atmosphere can possibly weaken the anchoring of Au on the USY support.

**Figure 4.** (**a**) TEM image and (**b**) particle size distribution of as-prepared 3 wt%-Au/USY zeolite.

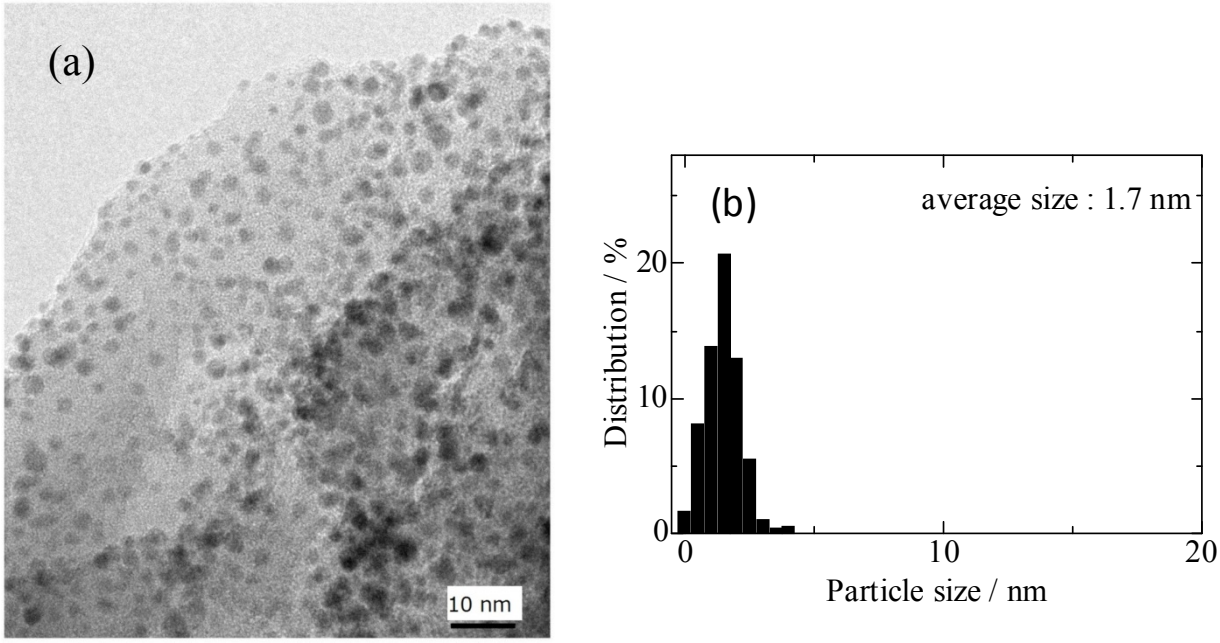


**Figure 5.** TEM images of Au/USY thermally treated in 6% $H_2$ diluted with Ar at (**a**) 473 K; (**b**) 773 K; (**c**) 973 K and (**d**) 1073 K. Samples were stored in the dark for more than one month.

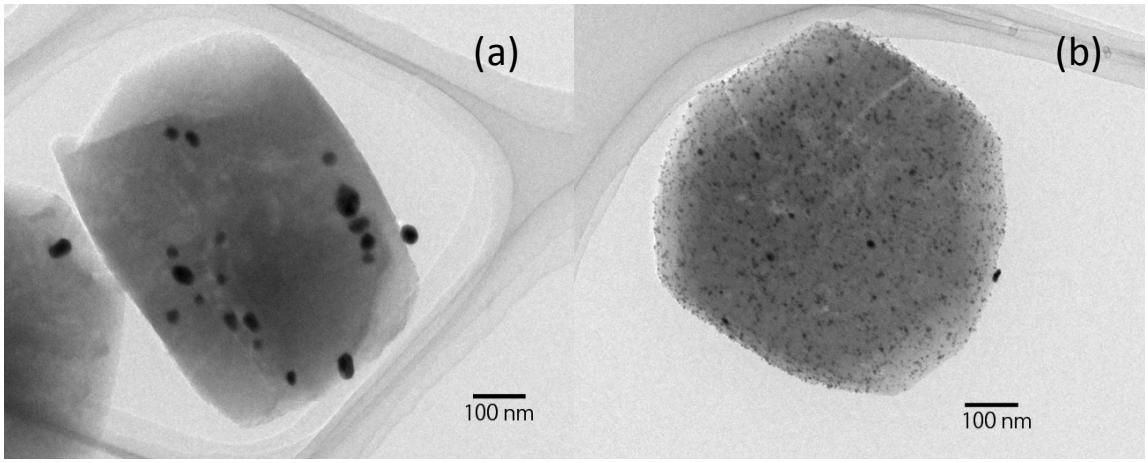

**Figure 5.** *Cont.*

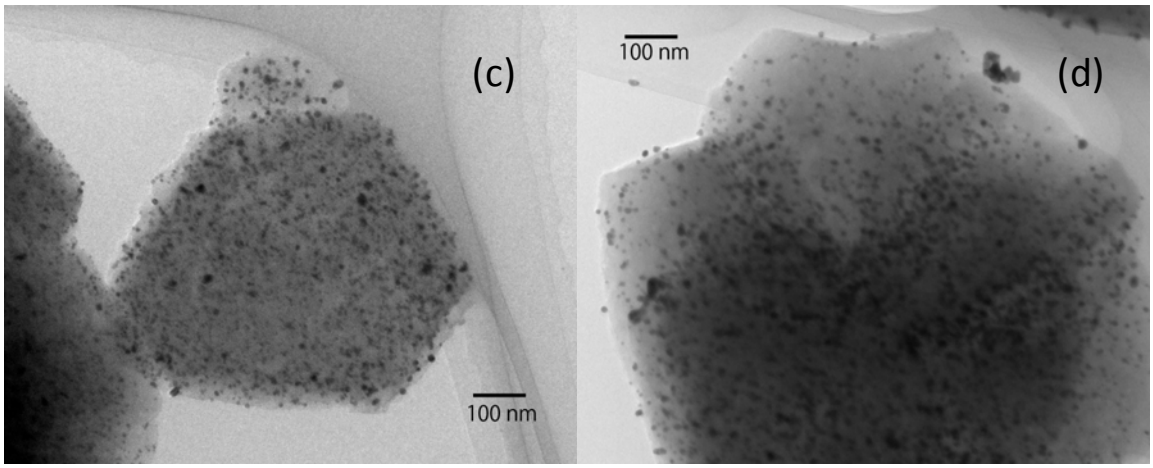


**Figure 6.** Distribution of Au particles in 3 wt% Au loaded on USY zeolites thermally treated in 6% $H_2$ diluted with Ar at (**a**) 473 K; (**b**) 773 K; (**c**) 973 K and (**d**) 1073 K.

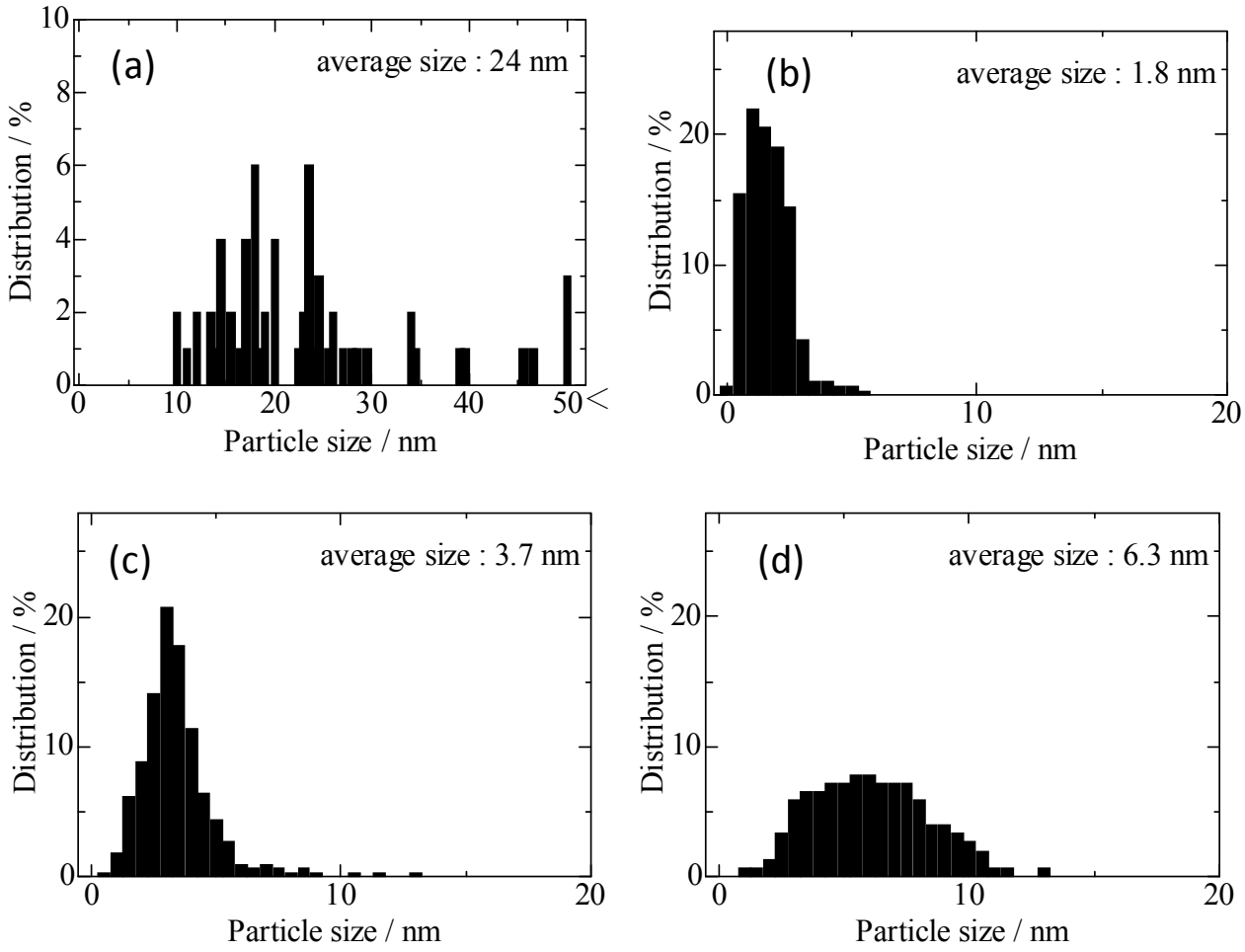


*2.4. IR Study of Adsorbed CO*

Low-temperature CO sorption experiments, monitored with the IR spectroscopy, were performed to determine the change in the dispersion of Au active sites by the thermal treatment temperature. It is

well known that CO is a useful probe for Lewis acid sites and is characterized by the narrow and well-resolved bands in the region 2250–2000 $cm^{-1}$. Figure 7 shows FTIR spectra of USY (parent, spectrum a) and Au/USY treated at 773 K in 6% $H_2$ diluted with Ar (spectrum b) recorded after the exposure to CO. The interaction of CO with the USY zeolite resulted in the appearance of the 2178 $cm^{-1}$ band, assigned to CO when it is bonded to Brønsted acid sites (Si(OH)Al groups) [20]. The same band can be detected in the spectra of Au zeolites with different Au dispersions. Adsorption of CO to the Au species dispersed in the USY zeolite, which was hydrogen-reduced at 773 K, is manifested by the appearance of two bands at 2128 and 2092 $cm^{-1}$. The latter band (at 2092 $cm^{-1}$) can be attributed to metallic Au species, whereas the former to Au cationic species [21–24]. The origin of the 2128 $cm^{-1}$ band was confirmed in the CO sorption experiments, carried out on the samples exposed to $O_2$ at 773 K (spectrum c). It was evident that the contact of the reduced samples with oxygen transformed the metallic species (disappearance of the 2092 $cm^{-1}$ band) to cationic Au oxide clusters (the 2128 $cm^{-1}$ band grew). Additionally, the oxide form of the Au species in the oxygen-treated zeolite was confirmed by the presence of the 2340 $cm^{-1}$ band for $CO_2$ that resulted from the oxidation of CO by the Au oxide species.

Figure 8 shows the FTIR spectra of CO adsorbed on the USY (parent) (spectrum a) and the Au/USY zeolites treated at 473 K in 6% $H_2$ diluted with Ar (spectrum b). The sample was stored in the dark for more than one month before conducting the IR measurements. Both the metallic and oxide forms of the Au species were detected by the presence of CO. Nevertheless, the intensity of the CO band attributed to the metallic species (at 2097 $cm^{-1}$) was considerably lower (threefold) than that for the Au/USY treated at 773 K. The same effect was found for cationic Au oxide species, the presence of which was confirmed by the appearance of two bands at 2131 and 2123 $cm^{-1}$. These findings confirmed the distinctly lower dispersion of the Au species (metallic and oxide forms) in the Au/USY zeolite treated with $H_2$ at 473 K compared to that reduced at 773 K. Poorer activity of the Au species was confirmed by the relatively lower intensity of the $CO_2$ band at 2340 $cm^{-1}$: the oxidation of CO to $CO_2$ was better facilitated on the dispersed oxide species than on the aggregated ones.

**Figure 7.** FTIR of adsorbed CO on (**a**) parent USY, (**b**) Au/USY treated in 6% $H_2$ at 773 K and (**c**) Au/USY treated in 6% $O_2$ at 773 K.

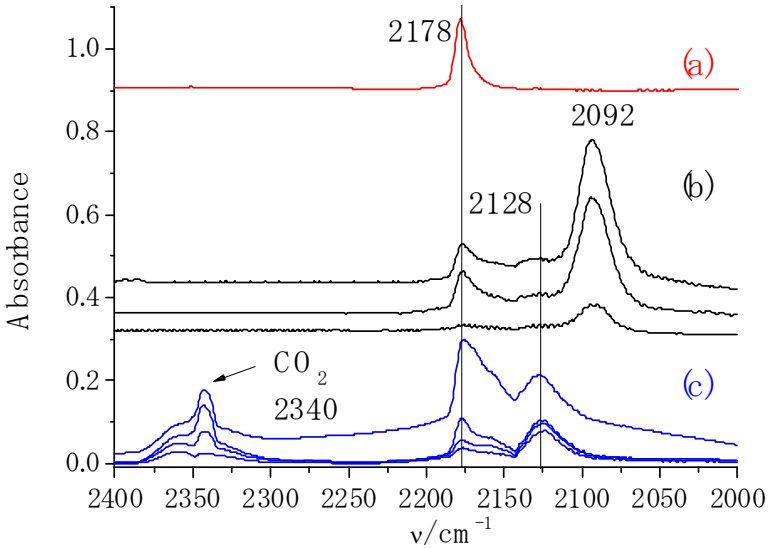

**Figure 8.** FTIR of adsorbed CO on (a) parent USY, (b) Au/USY treated in 6% $H_2$ at 473 K, and (c) Au/USY treated in 6% $O_2$ at 473 K.

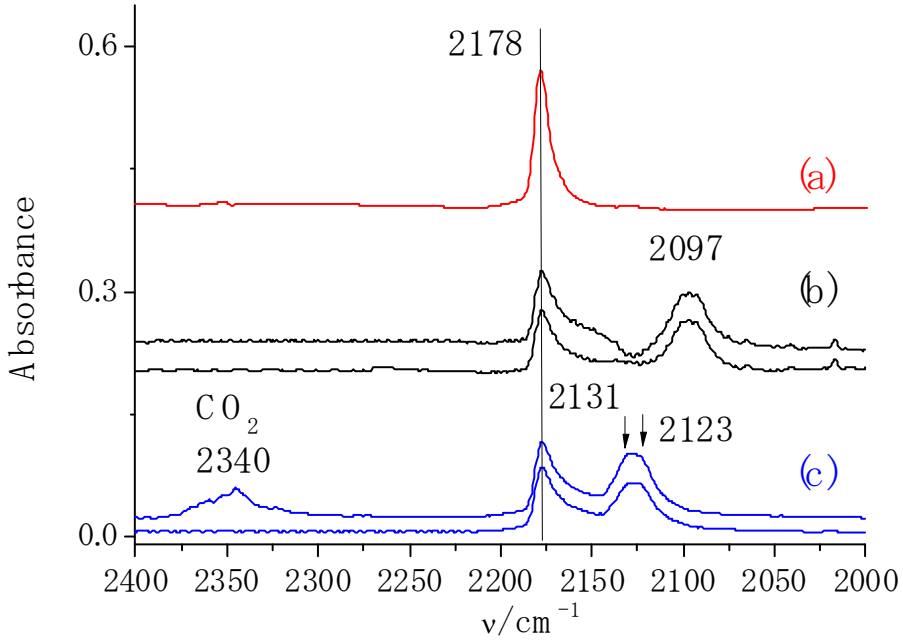


*2.5. Catalytic Performance in Aerobic Oxidation of Benzyl Alcohol*

Partial oxidation of benzyl alcohol in air has been tested for Au/Y-type zeolites, because the catalytic activity of Au in the reaction was sensitive to the size of the Au particles [25]. Here, the main product was benzaldehyde while the by-product was a small amount of benzyl benzoate. Formation of benzaldehyde was negligible when the USY zeolites without Au loading were used. Figure 9a shows that the conversion of benzyl alcohol and the yield of benzaldehyde increased with an increase in the calcination temperature. The highest activity (conversion and yield) was obtained when the catalyst was treated at 673–973 K. Similarly, the dependence of the catalytic activity on the thermal treatment temperature was observed in the homocoupling of phenylboronic acid [19]. The change in the particle size of Au was correlated with the catalytic activity, which increased as the size of the Au particles decreased. Figure 10 shows the data of the repetitive reaction over the Au/USY zeolite. Only slight deactivation was observed even after repeating the reaction for more than 10 times. The data indicated that the Au/USY catalyst exhibited recyclability and could be reused at least 12 times without any loss of catalytic activity.

Figure 9b shows the conversion and yield of the $Au/TiO_2$ catalyst prepared by the deposition-precipitation method. The maximum activity was obtained after the catalyst was thermally treated in 6% $H_2$ diluted with Ar at 573 K. As a result, the conversion of benzyl alcohol and the yield of benzyladehyde were 71% and 54% respectively, which were lower than those obtained with the Au/USY zeolite treated at 673–973 K.

**Figure 9.** Dependence of conversion and yield of benzaldehyde on calcination temperature of (**a**) 3 wt%-Au/USY zeolite and (**b**) 3 wt%-Au/$TiO_2$ treated in a stream of 6% $H_2$ dilute with Ar. Closed symbol: benzyl alcohol conversion; Open symbol: benzaldehyde yield.

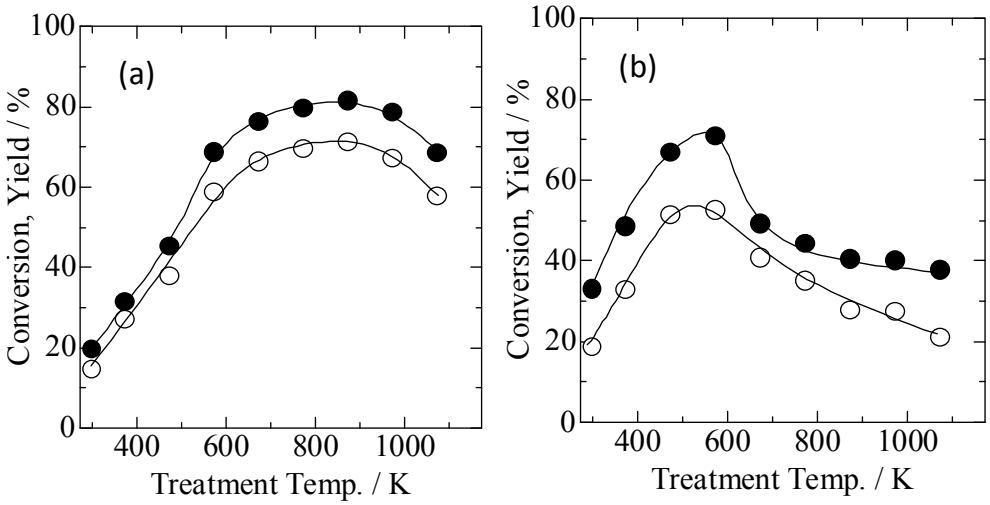


**Figure 10.** Catalytic performance of Au/USY zeolite treated at 773 K in 6% hydrogen in repetitive aerobic oxidation of benzyl alcohol.

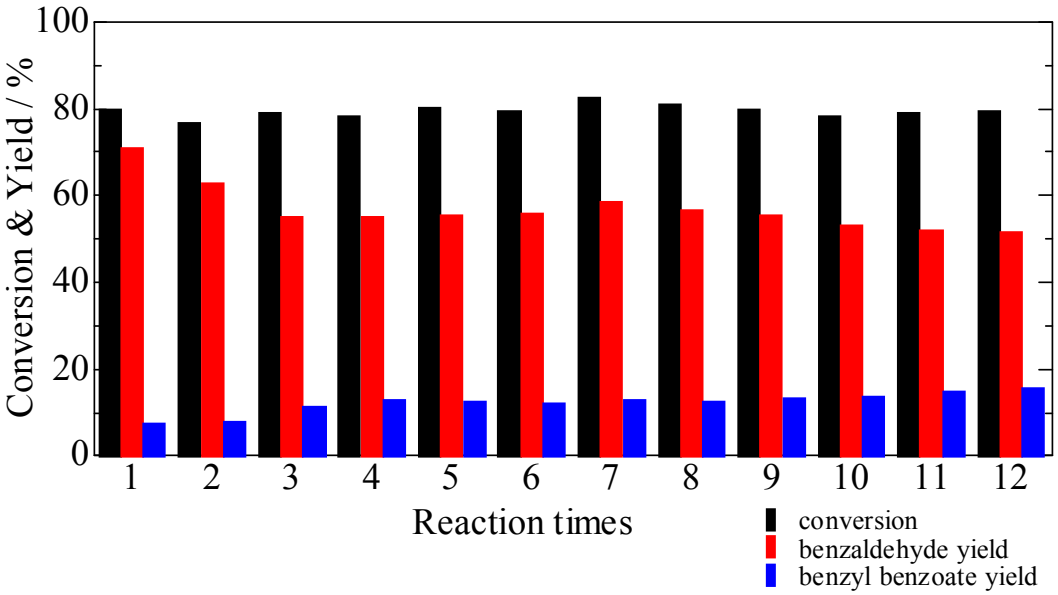


## 3. Experimental Section

### *3.1. Sample Preparation*

Au was loaded on zeolites using $HAuCl_4 \cdot 4H_2O$ (Wako Pure Chemical Industries, Ltd., Tokyo, Japan) as a precursor. The $NH_4$-type USY zeolite (purchased from Tosoh, Tokyo, Japan), HSZ-341NHA, $Si/Al_2$ = 7.7, 1 g) was immersed in an aqueous solution of $HAuCl_4$ (250 mL, $6.1 \times 10^{-4}$ mol $L^{-1}$), and the slurry was kept at 343 K for 1 h with constant stirring. The solution of $HAuCl_4$ was yellow but it decolorized during the treatment, while the zeolite became pale orange

within 1 h of the solution reaching 343 K. The Au-loaded USY zeolite was filtered, washed with deionized water, and air dried in an oven at 323 K. The Au loading was measured by an ICP spectrometer after the digestion of Au/USY zeolites in aqua regia. The typical amount of Au loading was 3 wt%. The resulting Au/USY zeolite was subsequently treated with a stream of 6% $H_2$ diluted with Ar at a given temperature for 30 min. The temperature ramping rate was 5 K $min^{-1}$. Au loading on the $CaNH_4^+$-type Y and $NH_4^+$-type Y zeolites was carried out analogously to the preparation of Au/USY zeolites. The $CaNH_4^+$-Y zeolite was prepared as reported elsewhere [26]. The concentration of Ca in the $CaNH_4^+$-Y was 1.0 mol $kg^{-1}$. The ZSM-5 (JRC-Z5-90NA(1), $Si/Al_2$ = 90), mordenite (JRC-Z-HM15, $Si/Al_2$ = 15), and β-zeolites (JRC-Z-B25(1) $Si/Al_2$ = 25) were three times ion-exchanged with an aqueous solution of 0.5 M $NH_4NO_3$ at 343 K to yield $NH_4^+$-form zeolites, prior to Au deposition. The deposition of Au was tried analogously on the $NH_4^+$-mordenite, β-type, and ZSM-5 zeolites for loading Au on Y-type zeolites. The precipitation-deposition method was employed for loading 3 wt% Au on $TiO_2$ (JRC-TIO-11, supplied by the Catalysis Society of Japan). First, 0.5 g of zeolite was added to a 100 mL solution of $HAuCl_4$ (Wako Pure Chemical Industries, Ltd., Tokyo, Japan) heated in a water bath at 343 K. The pH of the solution was adjusted to 6 by adding an ammonia solution (2.8%) with vigorous stirring. After adjusting the pH, the slurry was stirred for an additional 1 h. After filtration, the Au-loaded sample was thoroughly washed with deionized water until no $Cl^-$ was detected with $AgNO_3$ solution. Finally, the sample was dried in air at 323 K for 3 h.

### *3.2. TEM and XRD Data Collection and Analysis*

The TEM images were obtained using a HITACHI H-9000UHR microscope with an acceleration voltage of 300 kV. The crystalline structure of the Au zeolite was analyzed by XRD under ambient conditions using a Rigaku Ultima IV X-ray diffractometer with Cu Kα radiation. *In situ* XRD data was obtained using RIGAKU SmartLab equipped with a Johannson-type primary monochromator in the atmosphere of 3% $H_2$ diluted with Ar. The measurement was carried out in Bragg-Brentano geometry. Temperature ramping rate and scan speed were 5 K $min^{-1}$ and 4° $min^{-1}$, respectively.

### *3.3. IR Measurements and Analysis*

Prior to IR studies, the 3 wt%-Au/USY zeolites were pressed into thin discs (5 $mg/cm^2$) and thermally treated *in situ* in an IR cell under vacuum at 770 K for 1 h. Sorption of CO (Linde Gas Krakow, Poland 99.95%) was carried out to detect all types of reduced Au species. After collecting data for the reduced samples, the Au species were oxidized by bringing zeolites in contact with oxygen (obtained *in situ* by the thermal decomposition of $KMnO_4$) at either 773 K or 473 K (for respective samples) for 1 h. At this stage, the sorption of CO doses allowed us to discriminate between the oxidized and reduced species. In each experiment, CO was sorbed at 173 K until all the Au species were saturated (maximum intensities of the bands were observed at *ca.* 2130 and 2090 $cm^{-1}$). Additionally, the appearance of the 2178 $cm^{-1}$ band corresponding to the Si(OH)Al groups pointed to the complete saturation of all Au species. The IR spectra were recorded with a Bruker Tensor 27 spectrometer (equipped with an MCT detector) with a spectral resolution of 2 $cm^{-1}$.

### *3.4. Catalytic Reactions*

Partial oxidation of benzyl alcohol was carried out over Au/USY zeolites in air. The samples were pretreated in 6% $H_2$ at a given temperature before being used in the reaction. The treated samples were stored in the dark. Benzyl alcohol (1.0 mmol; Wako Pure Chemical Industries, Tokyo, Japan), $K_2CO_3$ (1.0 mmol; Wako Pure Chemical Industries, Tokyo, Japan), toluene (5 mL; Wako Pure Chemical Industries, Tokyo, Japan), and Au-loaded catalysts (10 mg) were used. The molar amount of Au was 1 mol% with respect to benzyl alcohol. A sample bottle (20 mL) was placed on a magnetic stirrer and subjected to vigorous stirring. The reaction was performed at 323 K under atmospheric conditions for 8 h. The reaction was quenched by adding acetone to the solution, and the solution was analyzed by Shimadzu 2010 Gas Chromatograph equipped with an InertCap Pure-WAX (30 m) capillary column. Tridecane was used as the internal standard for the quantitative analysis. For recycling tests, a fresh substrate was added to the catalyst after its precipitation at the bottom of the reactor and removal of the supernatant. The reaction was repeated under the aforementioned conditions.

## 4. Conclusions

Au was successfully loaded on the $NH_4$-form Y-type zeolite to yield 1.7-nm-sized $Au_2O_3$ along with the formation of $NH_4Cl$. The particle size of Au° generated through the thermal treatment of the $Au_2O_3$/USY zeolite in 6% $H_2$ diluted with Ar was highly dependent on the treatment temperature. The TEM analysis ascertained that the Au/USY zeolite treated at 473 K with subsequent preservation in air for one month resulted in the formation of 25-nm-sized Au particles. In contrast, formation of 1.8–3.7 nm Au particles was observed after thermal treatment at 773–973 K. This behavior agreed with the results of the XRD and IR analyses of the adsorbed CO. The intensity of the CO band, attributed to the metallic species in the Au/USY-773 K zeolite, was considerably higher (threefold) than that observed in the Au/USY-473 K zeolite. Moreover, the catalytic activity of the Au/USY zeolites in the partial oxidation of benzyl alcohol showed good correlation with the Au dispersion. The highest activity was attained with the Au/USY treated at 773–973 K. The simplicity of the technique used for Au loading is worth emphasizing: stirring a solution of $HAuCl_4$ and $NH_4$-type USY zeolites at 343 K afforded $Au_2O_3$. This study showed the possibility of regulating the size of Au particles by employing USY zeolites.

## Acknowledgments

This research was partially supported by the Ministry of Education, Science, Sports and Culture, Grantin-Aid for Scientific Research (C), 24560946. K. Góra-Marek acknowledges Grant No. 2011/01/B/ST5/00915 from the National Science Centre, Poland.

## References

1. Haruta, M. Size- and support-dependency in the catalysis of gold. *Catal. Today* **1997**, *36*, 153–166.
2. Daniel, M.C.; Astruc, D. Gold nanoparticles Assembly, supramolecular chemistry, quantum-size-related properties, and applications toward biology, catalysis, and nanotechnology. *Chem. Rev.* **2004**, *104*, 293–346.

3. Tsukuda, T.; Tsunoyama, H.; Sakurai, H. Aerobic Oxidations Catalyzed by Colloidal Nanogold. *Chem. Asian J.* **2011**, *6*, 736–748.
4. Haruta, M.; Date, M. Advances in the catalysis of Au nanoparticles. *Appl. Catal. A* **2001**, *222*, 427–437.
5. Sardar, R.; Funston, A.M.; Mulvaney, P.; Murray, R.W. Gold Nanoparticles: Past, Present, and Future. *Langmuir* **2009**, *25*, 13840–13851.
6. Corma, A.; Garcia, H. Supported gold nanoparticles as catalysts for organic reactions. *Chem. Soc. Rev.* **2008**, *37*, 2096–2126.
7. Veith, G.M.; Lupini, A.R.; Rashkeev, S.; Pennycook, S.J.; Mullins, D.R.; Schwartz, V.; Bridges, C.A.; Dudney, N.J. Thermal stability and catalytic activity of gold nanoparticles supported on silica. *J. Catal.* **2009**, *262*, 92–101.
8. Okumura, M.; Nakamura, S.; Tsubota, S.; Nakamura, T.; Azuma, M.; Haruta, M. Chemical vapor deposition of gold on $Al_2O_3$, $SiO_2$, and $TiO_2$ for the oxidation of CO and of $H_2$. *Catal. Lett.* **1998**, *51*, 53–58.
9. Zanella, R.; Giorgio, S.; Henry, C.R.; Louis, C. Alternative methods for the preparation of gold nanoparticles supported on $TiO_2$. *J. Phys. Chem. B* **2002**, *106*, 7634–7642.
10. Zanella, R.; Giorgio, S.; Shin, C.H.; Henry, C.R.; Louis, C. Characterization and reactivity in CO oxidation of gold nanoparticles supported on $TiO_2$ prepared by deposition-precipitation with NaOH and urea. *J. Catal.* **2004**, *222*, 357–367.
11. Tsubota, S.; Cunningham, D.; Bando, Y.; Haruta, M. CO Oxidation over Gold Supported on $TiO_2$. *Stud. Surf. Sci. Catal.* **1993**, *77*, 325–328.
12. Li, G.; EdwardS, J.; Carley, A.F.; Hutchings, G.J. Direct synthesis of hydrogen peroxide from $H_2$ and $O_2$ using zeolite-supported Au catalysts. *Catal. Today* **2006**, *114*, 369–371.
13. Guillemot, D.; Borovkov, V.Y.; Kazansky, V.B.; PolissetThfoin, M.; Fraissard, J. Surface characterization of Au/HY by Xe-129 NMR and diffuse reflectance IR spectroscopy of adsorbed CO. Formation of electron-deficient gold particles inside HY cavities. *J. Chem. Soc.-Faraday Trans.* **1997**, *93*, 3587–3591.
14. Hojholt, K.T.; Laursen, A.B.; Kegnaes, S.; Christensen, C.H. Size-Selective Oxidation of Aldehydes with Zeolite Encapsulated Gold Nanoparticles. *Top. Catal.* **2011**, *54*, 1026–1033.
15. Lin, C.H.; Lin, S.D.; Lee, J.F. Chlorine residue in the Au/gamma-$Al_2O_3$ prepared by $AuCl_3$ impregnation—An EXAFS analysis. *Catal. Lett.* **2003**, *89*, 235–242.
16. Okumura, K.; Tomiyama, T.; Morishita, N.; Sanada, T.; Kamiguchi, K.; Katada, N.; Niwa, M. Evolution of strong acidity and high-alkane-cracking activity in ammonium-treated USY zeolites. *Appl. Catal. A* **2011**, *405*, 8–17.
17. Rodriguez-Reyes, J.C.F.; Friend, C.M.; Madix, R.J. Origin of the selectivity in the gold-mediated oxidation of benzyl alcohol. *Surf. Sci.* **2012**, *606*, 1129–1134.
18. Zhou, L.P.; Yu, W.J.; Wu, L.; Liu, Z.; Chen, H.J.; Yang, X.M.; Su, Y.L.; Xu, J. Nanocrystalline gold supported on NaY as catalyst for the direct oxidation of primary alcohol to carboxylic acid with molecular oxygen in water. *Appl. Catal. A* **2013**, *451*, 137–143.
19. Okumura, K.; Murakami, C.; Oyama, T.; Sanada, T.; Isoda, A.; Katada, N. Formation of nanometer-sized Au particles on USY zeolites under hydrogen atmosphere. *Gold Bull.* **2012**, *45*, 83–90.

20. Sadowska, K.; Gora-Marek, K.; Datka, J. Hierarchic zeolites studied by IR spectroscopy: Acid properties of zeolite ZSM-5 desilicated with NaOH and NaOH/tetrabutylamine hydroxide. *Vib. Spectrosc.* **2012**, *63*, 418–425.
21. Grunwaldt, J.-D.; Maciejewski, M.; Becker, O.S.; Fabrizioli, P.; Baiker, A. Comparative Study of $Au/TiO_2$ and $Au/ZrO_2$ Catalysts for Low-Temperature CO Oxidation. *J. Catal.* **1999**, *186*, 458–469.
22. Venkov, T.; Fajerwerg, K.; Delannoy, L.; Klimev, H.; Hadjiivanov, K.; Louis, C. Effect of the activation temperature on the state of gold supported on titania: An FT-IR spectroscopic study. *Appl. Catal. A* **2005**, *301*, 106–114.
23. Lee, J.Y.; Schwank, J. Infrared Spectroscopic Study of NO Reduction by $H_2$ on Supported Gold Catalysts. *J. Catal.* **1986**, *102*, 207–215.
24. Debeila, M.A.; Coville, N.J.; Scurrell, M.S.; Hearne, G.R. DRIFTS studies of the interaction of nitric oxide and carbon monoxide on $Au\text{-}TiO_2$. *Catal. Today* **2002**, *72*, 79–87.
25. Zahmakiran, M.; Ozkar, S. The preparation and characterization of gold(0) nanoclusters stabilized by zeolite framework: Highly active, selective and reusable catalyst in aerobic oxidation of benzyl alcohol. *Mater. Chem. Phys.* **2010**, *121*, 359–363.
26. Noda, T.; Suzuki, K.; Katada, N.; Niwa, M. Combined study of IRMS-TPD measurement and DFT calculation on Bronsted acidity and catalytic cracking activity of cation-exchanged Y zeolites. *J. Catal.* **2008**, *259*, 203–210.